Influence of the second cladding on the properties of four-layer large flattened mode fibers

Chujun Zhao
Chinese Academy of Sciences
Shanghai Institute of Optics and Fine Mechanics
National Laboratory on High Power Laser and Physics
Shanghai 201800, China
and
Electronics Technology Group Corporation
No. 23 Research Institute
Shanghai 200437, China
E-mail: c_j_zhao@yahoo.com.cn

Yunxia Ye
Zhixiang Tang
Dianyuan Fan
Chinese Academy of Sciences
Shanghai Institute of Optics and Fine Mechanics
National Laboratory on High Power Laser and Physics
Shanghai 201800, China

Guanghui Chen
Wei Mu
Electronics Technology Group Corporation
No. 23 Research Institute
Shanghai 200437, China

Abstract. A theoretical method to analyze four-layer large flattened mode (LFM) fibers is presented. The influence of the second cladding on the properties of four-layer LFM fiber, including the fundamental and higher-order modal fields, effective area, bending loss, and dispersion, are studied by comparison. At the same time, the reasons for the different characteristics are considered. The obtained results indicate that the effective area of the four-layer LFM fiber is about 1.6 times larger than that of the conventional standard step-index fiber and the fibers have better bend-induced filtering ability than three-layer LFM fibers. [DOI: 10.1117/1.2779905]

Subject terms: large flattened mode (LFM) fiber; modal fields; effective area; bending loss.

Paper 060894RR received Nov. 16, 2006; revised manuscript received Apr. 5, 2007; accepted for publication Apr. 6, 2007; published online Sep. 21, 2007.

1 Introduction

The output power of a high-power optical fiber laser is limited by the onset of nonlinear effects, such as self-phase modulation, stimulated Raman scattering, and stimulated Brillouin scattering.[1] A common approach for scaling the power and pulse energy is to increase the core size of the fiber and selectively excite only the fundamental mode.[2] But there is an upper limit to the core diameter beyond which single-mode operation is not guaranteed. At numerical aperture (NA) lower than 0.06, furthermore, fibers begin to exhibit extremely high bend sensitivity, which imposes a practical lower limit on NA and hence an upper limit on core diameter.[3] Fortunately, many ways have been found to suppress higher-order lasing modes that allow designers to use even larger core diameters wherein essentially multimode fibers can be made to operate with a diffraction-limited beam quality. These techniques include suitably manipulating the fiber index and doping profiles,[4,5] using special cavity configurations,[6,7] tapering the fiber ends,[8] adjusting the seed launch conditions,[9] and coiling the fiber to induce substantial bend loss for all transverse modes other than the fundamental.[10]

The magnitude of nonlinearity in an optical fiber depends on the nonlinear refractive index coefficient of the fiber, the power in the optical fiber, and the mode confinement. The effective nonlinear coefficient of a fiber can be defined as n_{cl}/A_{eff}, where n_{cl} is the nonlinear refractive index coefficient and A_{eff} is the effective core area. The nonlinear refractive index coefficient of a fiber depends on the fiber material, and as such, it is almost the same for all silica-based fibers. Thus, the nonlinearity of the fiber can be reduced by increasing A_{eff}. The large flattened mode (LFM) optical fiber, firstly proposed by Ghatak et al. in 1999, has homogenous modal field in the central region.[11] This design can increase the effective area, which has been discussed and demonstrated at Lawrence Livermore National Laboratory.[11,12]

LFM fiber is a very promising candidate for high-power fiber lasers and amplifiers for its large effective area and flat-top fundamental modal field output. Previously, three-layer LFM fibers have been discussed in detail.[11–13] For the four-layer LFM fibers, some properties have been discussed earlier, in Ref. 14. Here we will discuss the influence of the second cladding on the properties of LFM fibers in more detail. We will present a generalized method to analyze the four-layer LFM fibers. The formulations to analyze the LFM fibers are deduced in Sec. 2. In Sec. 3, the influence

of the second cladding on the properties of the four-layer LFM fibers is studied in detail. Last, the main results obtained in the paper are summarized.

2 Theoretical Analyses

The properties of the fiber are evaluated with a scalar-wave analysis. The adequacy of this analysis is well established for fibers with small index variations with transverse dimensions. Assuming that fields are time-harmonic and travel in the $+z$ direction, the expressions for electric fields in a cylindrical coordinate system (r,Φ,z) are given by

$$\vec{E}(r,\phi,z)=\psi(r,\phi)\begin{Bmatrix}\hat{a}_x\\ \hat{a}_y\end{Bmatrix}\exp j(wt-\beta z)\exp(-\alpha z), \tag{1a}$$

$$\vec{H}(r,\phi,z)=Y_0 n(r)\hat{a}_z\times\vec{E}(r,\phi,z), \tag{1b}$$

where $\vec{E}$ is the transverse electric field, $\vec{H}$ is the transverse magnetic field, $\Psi(r,\Phi)$ is a scalar function describing the transverse distribution of fields, β is the propagation constant, w is the radian frequency of the light, α is the attenuation constant, $n(r)$ is the refractive index as a function of the radial coordinate, Y_0 is the free-space admittance, and $\hat{a}_x$, $\hat{a}_y$ are unit vectors in the x and y directions, respectively.

In the i'th region with refractive index n_i, the function $\Psi(r,\Phi)$ is the solution of the following scalar-wave equation[14–16]:

$$\frac{1}{r}\frac{\partial}{\partial r}\left(r\frac{\partial\psi}{\partial r}\right)+\frac{1}{r^2}\frac{\partial^2\psi}{\partial\phi^2}+(k_0^2n_i^2-\beta^2)\psi=0, \tag{2}$$

where $k_0=2\pi/\lambda$, and λ is the wavelength. For the four-layer cylindrical optical fiber, dropping the z- and Φ-dependent terms, which are common to solutions in all regions, and using the method of separation of variables, the solution to Eq. (2) is obtained as

$$\psi=\begin{cases}AZ_{n1}(k_1r)\cos n\phi, & r<r_1\\ [BZ_{n2}(k_2r)+C\bar{Z}_{n2}(k_2r)]\cos n\phi, & r_1<r<r_2\\ [DZ_{n3}(k_3r)+E\bar{Z}_{n3}(k_3r)]\cos n\phi, & r_2<r<r_3,\\ FZ_{n4}(k_4r)\cos n\phi, & r<r_3\end{cases} \tag{3}$$

where A, B, C, D, E, and F are constant amplitude coefficients. In the analysis, $n_{eff}=\beta/k_0$,

$$k_i=k_0(|n_i^2-n_{eff}^2|)^{1/2},$$

$$Z_{ni}=\begin{cases}J_n, \beta<n_i\\ I_n, \beta>n_i\end{cases},$$

$$\bar{Z}_{ni}=\begin{cases}Y_n, \beta<n_i\\ K_n, \beta>n_i\end{cases}, \quad J_n, Y_n,$$

are the Bessel functions of order n, and I_n, K_n are the modified Bessel functions of order n. The i'th layer has a radius r_i and a refractive index $n_i(i=1,2,3,4)$. $i=1$ corresponds to the central core region, while $i=2,3$, and 4 refer to cladding layers. The outer cladding layer $(i=4)$ is assumed to extend to infinity in the radial direction.

The boundary conditions at $r=r_i(i=1,2,3)$ require merely the continuity of ψ and $d\psi/dr$, so we can get

$$\frac{DZ_{n3}(k_3r_3)+E\bar{Z}_{n3}(k_3r_3)}{DZ'_{n3}(k_3r_3)+E\bar{Z}'_{n3}(k_3r_3)}=\frac{k_3Z_{n4}(k_4r_3)}{k_4\bar{Z}'_{n4}(k_4r_3)}, \tag{4}$$

where the amplitudes' coefficients can be calculated in terms of A:

$$C=\frac{k_2Z_{n1}(k_1r_1)Z'_{n2}(k_2r_1)-k_1Z'_{n1}(k_1r_1)Z_{n2}(k_2r_1)}{k_2\bar{Z}_{n2}(k_2r_1)Z'_{n2}(k_2r_1)-k_2\bar{Z}'_{n2}(k_2r_1)Z_{n2}(k_2r_1)}A,$$

$$B=\frac{AZ_{n1}(k_1r_1)-C\bar{Z}_{n2}(k_2r_1)}{Z_{n2}(k_2r_1)},$$

$$M=\frac{Bk_2Z'_{n2}(k_2r_2)+Ck_2\bar{Z}'_{n2}(k_2r_2)}{BZ_{n2}(k_2r_2)+C\bar{Z}_{n2}(k_2r_2)},$$

$$N=\frac{k_3\bar{Z}'_{n3}(k_3r_2)-M\bar{Z}_{n3}(k_3r_2)}{MZ_{n3}(k_3r_2)-k_3Z'_{n3}(k_3r_2)},$$

$$E=\frac{BZ_{n2}(k_2r_2)+C\bar{Z}_{n2}(k_2r_2)}{NZ_{n3}(k_3r_2)+\bar{Z}_{n3}(k_3r_2)},$$

$$F=\frac{DZ_{n3}(k_3r_3)+E\bar{Z}_{n3}(k_3r_3)}{Z_{n4}(k_4r_3)}, \quad D=EN.$$

Obviously, for the fundamental modal field to be absolutely flat in the region $|r|<r_1$, we must have $d\psi/dr=0$, $n_{eff}=n_1$. In the discussion, $n_4<n_1$, and thus the modal field distributions are

$$\psi=\begin{cases}A, & r<r_1\\ [BZ_{02}(k_2r)+C\bar{Z}_{02}(k_2r)], & r_1<r<r_2\\ [DZ_{03}(k_3r)+E\bar{Z}_{03}(k_3r)], & r_2<r<r_3\\ FK_0(k_4r), & r>r_3\end{cases}. \tag{5}$$

The corresponding transcendental equation can be deduced from Eq. (4).

To investigate the effective area of the LFM fibers, A_{eff} can be calculated from

$$A_{eff}=2\pi\frac{\left[\int_0^\infty\psi^2(r)r\,dr\right]^2}{\int_0^\infty\psi^4(r)r\,dr}, \tag{6}$$

where $\psi(r)$ is given by Eq. (5). The expression for the effective area is based on the so-called Petermann II definition.[17]

For the bending loss of the fiber, bend-induced mode distortion[18] has not been observed in experiment, so we did not consider it. Here, we used the method presented by

Snyder.[19] The fiber core and inner claddings are substituted by an equivalent current radiating as an antenna in an infinite medium of index equal to n_N, where n_N is the refractive index of the most external layer for an N-layer fiber. In this paper, $N=4$. To a first approximation and using the Maxwellian equation $\nabla \times \vec{H} = \vec{J} + jw\varepsilon\vec{E}$, it can be shown that the current density of the equivalent radiating antenna is given by the following expression:

$$\vec{J} = -jk_0(\epsilon_0/\mu_0)^{1/2}[n_N^2 - n^2(r)]\vec{E}(r), \tag{7}$$

where $\vec{E}(r)$ is the exact electric field of the fiber, ϵ_0 is the free-space dielectric constant, and μ_0 is the free-space permeability. As an approximation, it is sufficient to assume that this field is the same as the field of the straight fiber, provided that the bending radius is large enough compared with the fiber dimensions. The fiber is assumed to be bent at a constant radius R_c. The current amplitude I_{co} can be expressed as

$$I_{co} = -j2\pi k_0(\epsilon_0/\mu_0)^{1/2}\int_0^\infty [n_N^2 - n^2(r')]\psi(r') I_0[k_0(n_{eff}^2 - n_N^2 r')^{1/2}]r'\,\mathrm{d}r'. \tag{8}$$

Following the steps of Snyder, the radiated power is expressed as:

$$P_{rad} = \frac{\pi}{2\lambda} n_N(\mu_0/\epsilon_0)^{1/2} R_c |I_{co}|^2 F_{rad} \times \exp\left\{-\frac{2k_0 n_N R_c}{3}\left[\left(\frac{n_{eff}}{n_N}\right)^2 - 1\right]^{3/2}\right\}, \tag{9}$$

where

$$F_{rad} = \frac{1}{(n_{eff}^2 - n_N^2)^{1/2}} \left\{\frac{3\lambda}{8n_N R_c[(n_{eff}/n_N)^2 - 1]^{1/2}[2(n_{eff}/n_N)^2 + 1]}\right\}^{1/2}.$$

Thus, the loss coefficient is calculated as:

$$\gamma = P_{rad}/2\pi R_c P(0), \tag{10}$$

where $P(0) = \pi(\epsilon_0/\mu_0)^{1/2}\int_0^\infty n(r)|\psi(r)|^2 r\,\mathrm{d}r$ is the power carried by the wave at the fiber input.

3 Results and Discussion

If we add a second cladding to the three-layer LFM fiber, the three-layer LFM fiber will become a four-layer LFM one. In this paper, we will discuss the kind of four-layer LFM fiber and the influence of the second cladding on its properties. We define three parameters: $p = r_3/r_2$, $\Delta_i' = (n_i^2 - n_1^2)/2n_i^2$, $\Delta_i = (n_i^2 - n_4^2)/2n_i^2$ $(i = 1,2,3,4)$. In the calculation, $r_1 = 12$ μm, $r_2 = 15$ μm, $\lambda = 1.06$ μm, $\Delta_1 \approx 0.07\%$, and $\Delta_2 \approx 0.13\%$. The introduction of Δ_3' is just to classify the four-layer LFM fibers, and here there are two kinds: $\Delta_3' > 0$ and $\Delta_3' < 0$. In the following discussion, we will examine the fibers with different Δ_3. The refractive index profiles of the fibers are shown in Fig. 1. The fibers all have depressed index cores. Following Eq. (5), we can get the modal field distribution of the corresponding LFM fiber by adjusting p and Δ_3.

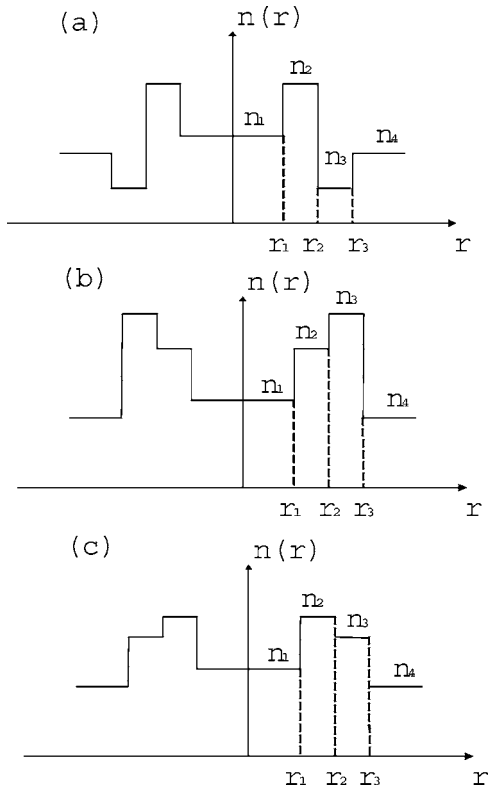

Fig. 1 Schematic of the refractive index profiles of the discussed fibers with (a) $\Delta_3 < 0$; (b) $\Delta_3 > 0$ and $n_2 < n_3$; (c) $\Delta_3 > 0$; and $n_2 > n_3$.

3.1 *Modal Fields*

The four-layer LFM fiber has large core size compared with conventional step-index fiber, and it is not single mode. In this work, we will discuss the four lowest modes of the fiber: LP_{01}, LP_{11}, LP_{21}, and LP_{02}. With proper Δ_3 and p, the LFM fiber shows flat fundamental field in the central region, but for the LP_{11}, LP_{21}, and LP_{02} modes, the modal fields vary, as shown in Fig. 2.

For the flat-top fundamental modal field, this can be explained as follows: When $\Delta_3 = -0.002$, -0.0015, and -0.001, n_2 is the largest, as shown in Fig. 1(a). Light cannot be confined into the core region well, and part of the light energy leaks into the first cladding. Meanwhile, $n_2 > n_3$ makes the light energy well confined in the first cladding. Energy redistribution takes place as light propagates along the fiber. A stable homogeneous intensity distribution of the fundamental mode would form in the core at last. When $\Delta_3 = 0.001$, 0.0015, and 0.002, $n_3 > n_1$. If $\Delta_3 = 0.0015$, 0.002, n_3 is the largest, as shown in Fig. 1(b). If $\Delta_3 = 0.001$, n_2 is the largest, as shown in Fig. 1(c). The reason is that forming the flat-top fundamental mode is the same as $\Delta_3 < 0$. The light energy leaks into the first and the second claddings, and the flat-top fundamental mode is formed.

It also can be found that the modal fields are nearly the same for different Δ_3. By calculation, to maintain the flat-top fundamental mode, it can be determined that the in-

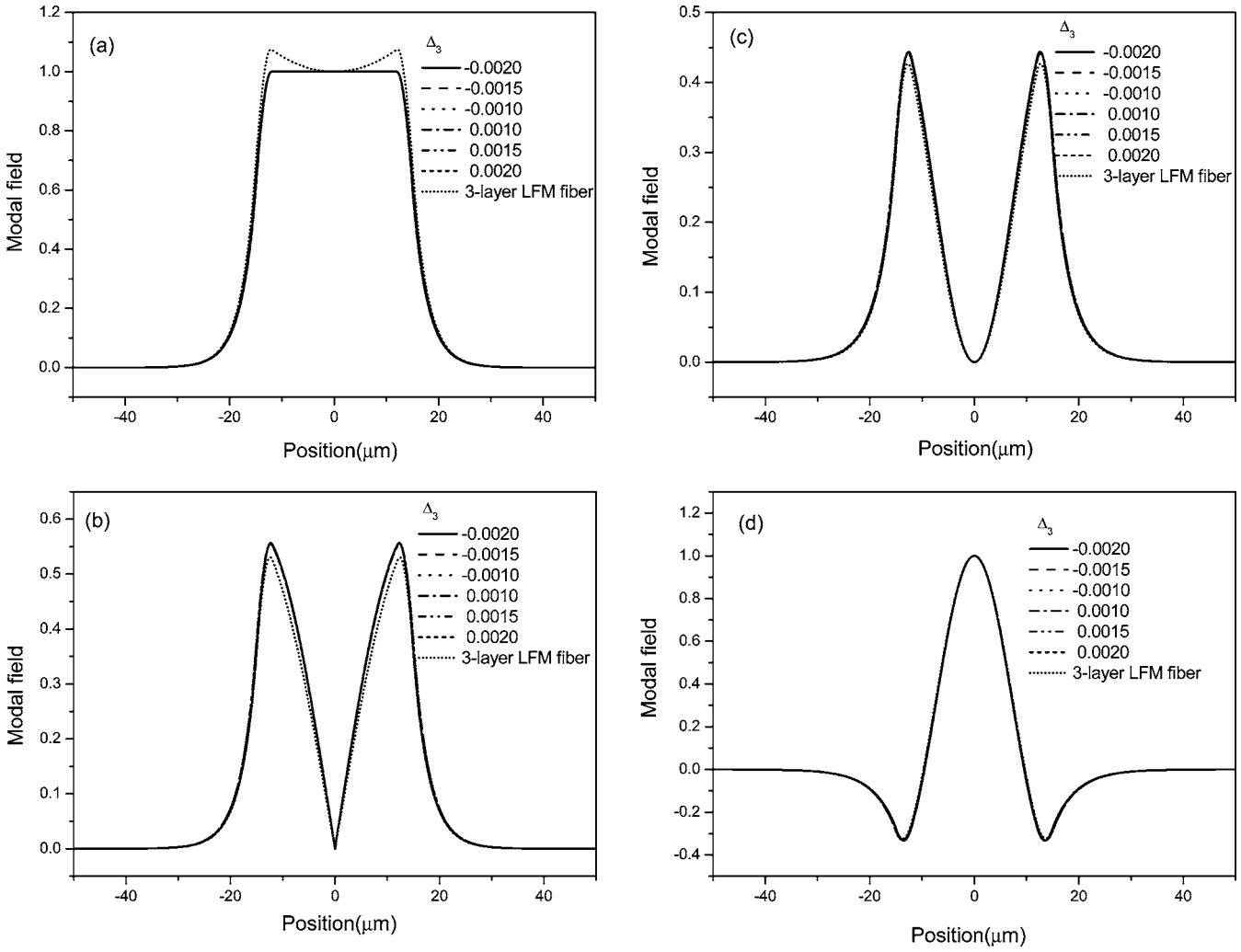

Fig. 2 Modal field distributions with different Δ_3: (a) LP_{01} modes, (b) LP_{11} modes, (c) LP_{21} modes, and (d) LP_{02} modes. The same characteristics for the three-layer LFM fiber are also given.

crease of Δ_3 leads to the increase of p if $\Delta_3<0$ and the decrease of p if $\Delta_3>0$, as shown in Fig. 3. Furthermore, the variation of p for $\Delta_3<0$ and $\Delta_3>0$ is small, which results in the small variation of modal fields. Figures 2(b) to 2(d) show the calculated field distribution for the LP_{11}, LP_{21}, and LP_{02} modes. The LP_{11} and LP_{21} modes have similar modal field distributions, having no intensity in the fiber center. Compared with the LP_{11} mode, the modal field of LP_{21} shifts towards the fiber border. LP_{02} mode has a similar modal field as the fundamental mode, but its field is much narrower, having more oscillations.

The modal fields of the three-layer LFM fiber, which has $r_1=12$ μm, $r_2=15$ μm, $n_1=1.458$, $n_2=1.459$, and $n_3=1.457$, are also plotted here. From the plots, it can be seen clearly that the three-layer LFM fiber has similar modal characteristics to the four-layer one.

3.2 *Effective Area*

Three-layer LFM fibers have a larger effective area, which has been previously demonstrated.[12] The four-layer LFM fiber also has a larger effective area compared with the conventional step-index fiber, as shown in Fig. 4. In this discussion, the conventional step-index fiber has core size r_3 and a flat refractive index of $\Delta_1\approx0.07\%$ across the entire core, and the outmost cladding has the same index as the LFM fibers. To maintain the flat-top mode, the value of p varies with different wavelength. For different Δ_3, the effective areas of the LFM fiber are nearly the same, and the effective area difference between conventional step-index fibers is also small. The effective area of the LFM fiber, however, is larger than the corresponding conventional step-index one, as shown in Fig. 4.

When $\Delta_3<0$, p decreases with increasing wavelength, which means r_3 decreases for the fixed r_2. For the conventional step-index fiber, smaller core size corresponds to smaller effective area,[19] so the effective area decreases with the increasing wavelength. But for the LFM fiber, the effective area increases with the increasing wavelength because the increase of the effective area outweighs the decrease of r_3. The large effective area of the LFM fiber can be explained by the flat-top modal field resulting from the light energy in the depressed core leaking into the claddings. For the small variation of p, the effective area changes little.

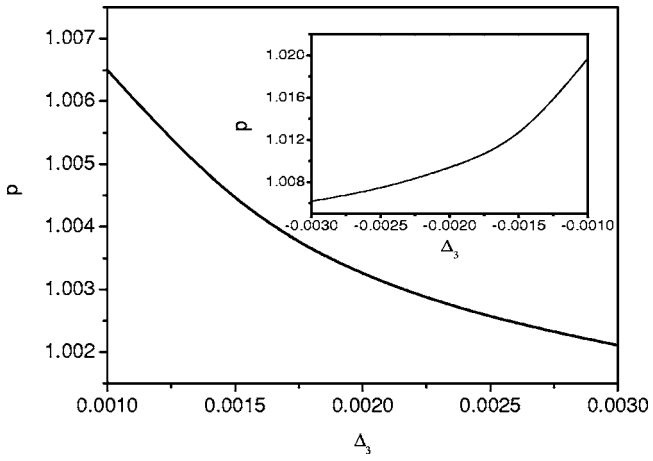

Fig. 3 Δ_3 versus p when $\Delta_3>0$, with the case $\Delta_3<0$ shown in the insert.

While $\Delta_3>0$, the effective areas of the two kinds of fibers all increase with increasing wavelength, as shown in Fig. 4(b). Unlike the case $\Delta_3<0$, p increases with increasing wavelength, which means that r_3 increases, too. For the conventional step-index fiber, larger core size corresponds to larger effective area, so the effective area increases with the increasing wavelength. For the LFM fiber, the flat-top fundamental field plays an important role for the large effective area.

To investigate the improved effective area quantitatively, it can be seen from Fig. 4 that the effective area of the four-layer LFM fiber can be increased by a factor of about 1.6 for the cases $\Delta_3<0$ and $\Delta_3>0$ compared with the conventional step-index one. Compared with the three-layer LFM fiber, as mentioned in Sec. 3.1, the four-layer LFM fiber has a larger effective area at shorter wavelength and a smaller effective area at longer wavelength.

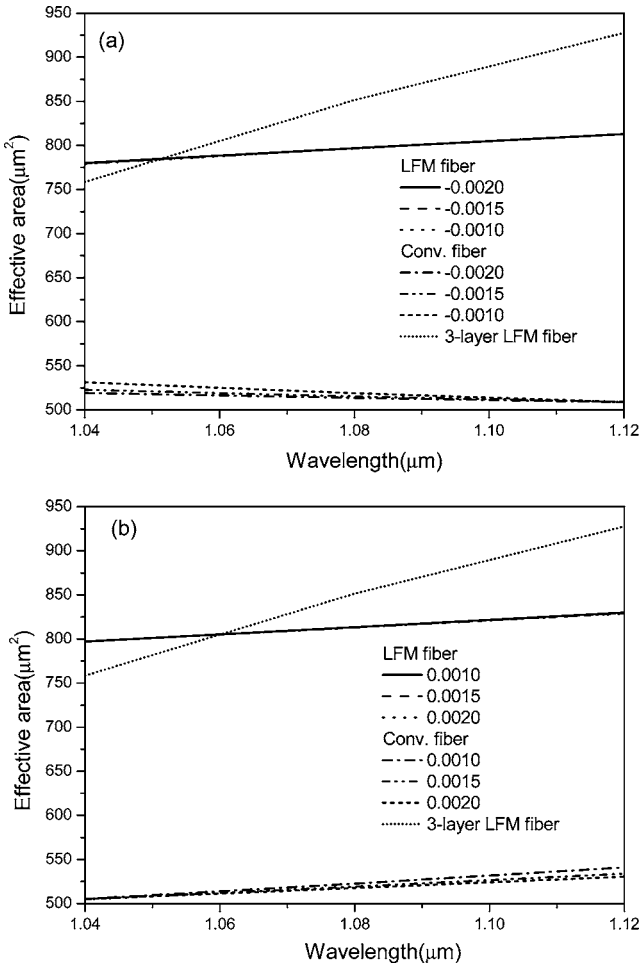

Fig. 4 Effective area comparisons between the four-layer LFM fiber and the conventional step-index fiber with (a) $\Delta_3<0$; (b) $\Delta_3>0$. The same characteristics for the three-layer LFM fiber are also given.

3.3 *Bending Loss*

The LFM fiber is an ideal candidate for the high-power fiber laser for its large effective area. With power scaling, maintaining high beam quality is imperative, while bending the fiber provides the easiest method to suppress the higher-order modes. Figure 5 shows the relationship of the bending loss of the LP_{01} mode with different Δ_3. With increasing bending radius, the bending loss decreases exponentially, which can be understood from Eq. (9) and Eq. (10) in Sec. 2. It also can be found that the bending losses of the fibers with different Δ_3 are nearly the same. This can be explained as follows: For these LFM fibers, they have the same n_{eff} for the LP_{01} mode, so the difference between bending losses originates from the fiber refractive index profile and the fiber geometry, as can be expected from Eqs. (5) to (8). Typically, large-core fibers show the most pronounced bending effects, while the small-diameter fibers show the least. p varies little for the cases $\Delta_3<0$ and $\Delta_3>0$, and thus r_3 varies little, so the bending losses do not change much.

The fundamental quantities required for understanding LFM fibers are the losses associated with the desired fundamental mode, LP_{01}, and the higher-order modes. For these higher-order modes, LP_{11} is the mode with the lowest susceptibility to bending loss. Thus, it is instructive to investigate the interplay of modal discrimination, defined here as the difference between loss of LP_{11} (γ_{11}) and LP_{01} (γ_{01}). Figure 6 shows the variation of the modal discrimination versus the bending radius for the four-layer LFM fibers. The modal discrimination of the three-layer LFM fiber discussed in Sec. 3.1 is also plotted here. If $\Delta_3<0$, the modal discriminations of the fibers are nearly the same. For the cases $\Delta_3>0$, the modal discriminations are also nearly the same and greater than the cases of $\Delta_3<0$. It also can be found that the four-layer LFM fibers have better modal discriminations than the three-layer LFM fibers at a fixed bending radius.

Figure 7 shows the variation of the modal discrimination versus γ_{01}. The modal discrimination of the three-layer LFM fiber[12] is also plotted here. It can be seen that the modal discrimination increases with increasing γ_{01}. If we set $\gamma_{01}=0.1$ dB/m and we assume that 1 dB/m discrimination can discriminate the LP_{01} from LP_{11}, it can be seen that all the four-layer LFM fibers can operate in single mode. But the three-layer LFM fiber has lower modal discrimina-

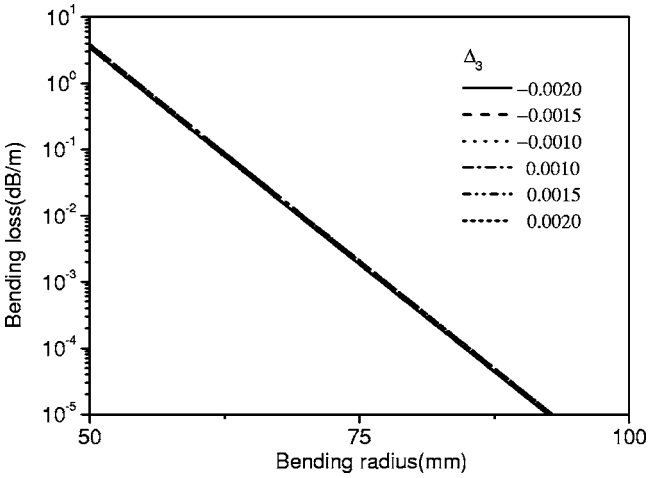

Fig. 5 Bending losses of the LP_{01} modes versus bending radius with different Δ_3.

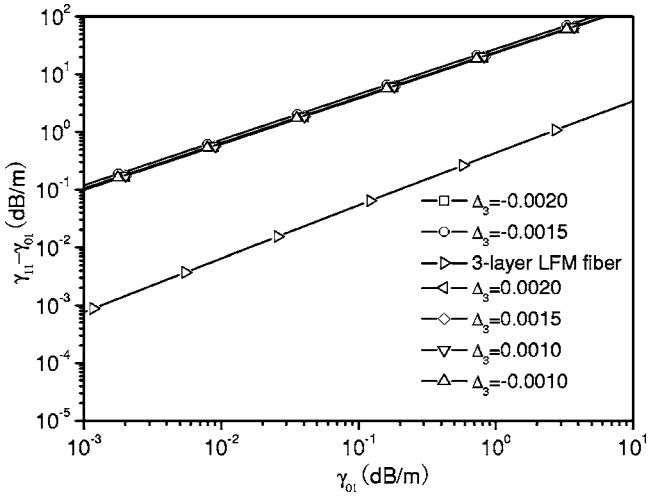

Fig. 7 Modal discriminations versus bending loss of flat-top mode with different Δ_3 for four-layer LFM fibers, and the same characteristics for the three-layer LFM fiber.

tion ability. The calculation provides a conservative estimate of the bending loss. The influence of the rare earth doping is not discussed in this paper.

3.4 *Dispersion*

With propagation constants obtained by numerically solving Eq. (4), the group velocities (v_g) and waveguide dispersions (D_w) can be obtained as[20]:

$$v_g = \frac{dw}{d\beta} = -\frac{2\pi c}{\lambda^2}\frac{d\lambda}{d\beta},$$

$$D_w = \frac{d(v_g^{-1})}{d\lambda}.$$

We carried out waveguide dispersion calculation for the flat-top mode of the LFM fibers with different Δ_3, as shown in Fig. 8. For these fibers, the flat-top mode can be obtained at 1.06 μm, but at other wavelengths, the modal field is no longer flat-top. If $\Delta_3 = -0.002$, -0.0015, and -0.001, the waveguide dispersion is nearly the same. For the cases $\Delta_3 = 0.001$, 0.0015, and 0.002, the fibers have nearly the same values, too. By comparison, it can be seen clearly from Fig. 8 that and the fibers with $\Delta_3 > 0$ have larger dispersion than the cases $\Delta_3 < 0$. Furthermore, the discussed three-layer LFM fiber has smaller waveguide dispersion compared with the four-layer one.

4 Conclusions

In summary, we have presented the design method of four-layer LFM fibers. We mainly discuss the influence of the fiber's second cladding on the properties of the fiber. The results show that p, effective area, and bending loss vary little with different Δ_3. These fibers have flat-top fundamental modal fields, from which it can be understood that the light cannot be confined in the core region well. The comparison between the LFM fiber and the standard step-index fiber indicates that the LFM fiber has a larger effec-

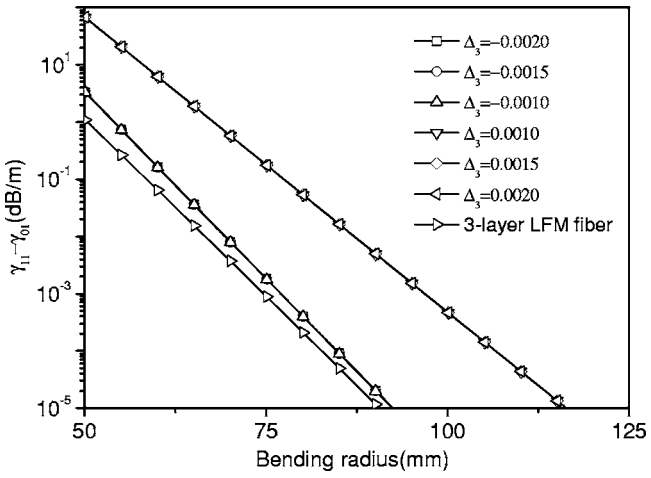

Fig. 6 Modal discriminations versus bending radius with different Δ_3 for four-layer LFM fibers, and the same characteristics for the three-layer LFM fiber.

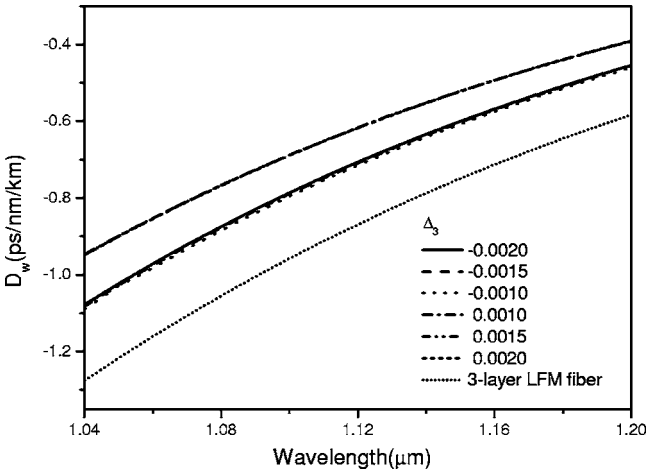

Fig. 8 Waveguide dispersion for the four-layer LFM fibers with different Δ_3, and the same characteristics for the three-layer LFM fiber.

tive area. Compared with the three-layer LFM fiber, the four-layer LFM fibers have a larger effective area at shorter wavelength and a smaller effective area at longer wavelength and have better bend-induced filtering ability. Furthermore, the feasibility is also given to suppress the higher-order modes via bending to realize a high-power, high beam quality fiber laser.

Acknowledgments

This work was partially supported by the Natural Science Foundation of China (Grant No. 10576012) and the National Key Basic Research Project of China (Grant No. 61359020201).

References

1. G. P. Agrawal, *Nonlinear Fiber Optics*, Academic, New York (1989).
2. M. E. Fermann, "Single-mode excitation of multimode fibers with ultrashort pulses," *Opt. Lett.* **23**, 52–54 (1998).
3. A. Tünnermann, T. Schreiber, F. Röser, A. Liem, S. Höfer, H. Zellmer, S. Nolte, and J. Limpert, "The renaissance and bright future of fibre lasers," *J. Phys. B* **38**, S681–S693 (2005).
4. H. L. Offerhaus, N. G. Broderick, D. J. Richardson, R. Sammut, J. Caplen, and L. Dong, "High-energy single-transverse-mode Q-switched fiber laser based on a multimode large-mode-area erbium-doped fiber," *Opt. Lett.* **23**, 1683–1685 (1998).
5. T. Bhutta, J. I. Mackenzie, D. P. Shepherd, and R. J. Beach, "Spatial dopant profiles for transverse-mode selection in multimode waveguides," *J. Opt. Soc. Am. B* **19**, 1539–1543 (2002).
6. U. Griebner, R. Koch, H. Schonnagel, and R. Grunwald, "Efficient laser operation with nearly diffraction-limited output from a diode-pumped heavily Nd-doped multimode fiber," *Opt. Lett.* **21**, 266–269 (1996).
7. U. Griebner and H. Schonnagel, "Laser operation with nearly diffraction-limited output from a YbYAG multimode channel waveguide," *Opt. Lett.* **24**, 750–752 (1999).
8. J. A. Alvarez-Chavez, A. B. Grudinin, J. Nilsson, P. W. Turner, and W. A. Clarkson, "Mode selection in high power cladding pumped fibre lasers with tapered section," *Conference on Lasers and Electro-Optics*, 247–248 (1999).
9. I. Zawischa, K. Plamann, C. Fallnich, H. Welling, H. Zellmer, and A. Tünnermann, "All-solid-state neodymium-based single-frequency master-oscillator fiber power-amplifier system emitting 5.5 W of radiationat 1064 nm," *Opt. Lett.* **24**, 469–471 (1999).
10. J. P. Koplow, D. A. V. Kliner, and L. Goldberg, "Single-mode operation of a coiled multimode fiber amplifier," *Opt. Lett.* **25**, 442–444 (2000).
11. A. K. Ghatak, I. C. Goyal, and R. Jindal, "Design of waveguide refractive index profile to obtain flat modal field," *Proc. SPIE* **3666**, 40–44 (1999).
12. J. W. Dawson, R. Beach, I. Jovanovic, B. Wattellier, Z. Liao, S. A. Payne, and C. P. J Barty, "Large flattened mode optical fiber for reduction of nonlinear effects in optical fiber lasers," *Proc. SPIE* **5335**, 132–139 (2004).
13. C. J. Zhao, R. W. Peng, Z. X. Tang, Y. X. Ye, L. Shen, and D. Y. Fan, "Modal fields and bending loss analyses of three-layer large flattened mode fibers," *Opt. Commun.* **266**, 175–180 (2006).
14. R. K. Varshney, A. K. Ghatak, I. C. Goyal, and S. A. C, "Design of a flat field fiber with very small dispersion slope," *Opt. Fiber Technol.* **9**, 189–198 (2003).
15. H. T. Hattori and A. Safaai-Jazi, "Fiber designs with significantly reduced nonlinearity for very long distance transmission," *Appl. Opt.* **37**, 3190–3197 (1998).
16. S. F. Mahmoud and A. M. Kharbat, "Transmission characteristics of acoaxial optical fiber line," *J. Lightwave Technol.* **11**, 1717–1720 (1993).
17. K. Petermann, "Constraints for fundamental mode spot size for broadband dispersion-compensated single-mode fibers," *Electron. Lett.* **19**, 712–714 (1983).
18. J. M. Fini, "Bend-resistant design of conventional and microstructure fibers with very large mode area," *Opt. Express* **14**, 69–81 (2006).
19. A. W. Snyder and J. D. Love, *Optical Waveguide Theory*, Chapman and Hall, London (1983).
20. B. E. A. Saleh and M. C. Teich, *Fundamentals of Photonics*, John Wiley & Sons, New York (1991).

Chujun Zhao received his BS and MS degrees in physics from Hunan University, Changsha, China, in 2002 and 2005, respectively. He is currently working toward a PhD degree in optics at the Shanghai Institute of Optics and Fine Mechanics, Chinese Academy of Sciences, Shanghai, China. His research interests are optical waveguides in high-power fiber lasers and amplifiers.

Yunxia Ye received her BS and MS degrees from Jiangsu University, Zhenjiang, China, in 1999 and 2002, respectively. She is currently working toward a PhD degree in optical engineering at the Shanghai Institute of Optics and Fine Mechanics, Chinese Academy of Sciences, Shanghai, China. Her research interests are solid-state and liquid-state laser theory.

Zhixiang Tang received his BS and MS degrees from Xiangtan University, Xiangtan, China, in 2001 and 2004, respectively. He is currently working toward a PhD degree in optical engineering at the Shanghai Institute of Optics and Fine Mechanics, Chinese Academy of Sciences, Shanghai, China. His research interests are laser propagation theory and metamaterials.

Dianyuan Fan is a professor at the Shanghai Institute of Optics and Fine Mechanics, Chinese Academy of Sciences, Shanghai, China. His major research areas include high-power solid-state laser research and application, and laser propagation theory and application, and interactions between lasers and materials.

Guanghui Chen is a professor at the Electronics Technology Group Corporation No. 23 Research Institute, Shanghai, China. His major research areas are fiber optics and related areas.

Wei Mu is an advanced engineer at the Electronics Technology Group Corporation No. 23 Research Institute, Shanghai, China. Her major research areas are fiber optics and related areas.